Effects of (5'S)-5',8-cyclo-2'-deoxyadenosine on the base excision repair of oxidatively generated clustered DNA damage. A biochemical and theoretical study.

Journal:	*Organic & Biomolecular Chemistry*
Manuscript ID:	OB-ART-05-2014-001089.R2
Article Type:	Paper
Date Submitted by the Author:	28-Aug-2014

Complete List of Authors:	Karwowski, Boleslaw; Medical University, Food Science Belone, Sophie; University of Oxford, DNA Damage Group, CRUK/MRC Oxford Institute for Radiation Oncology O'Neill, Peter; University of Oxford, DNA Damage Group, CRUK/MRC Oxford Institute for Radiation Oncology Lomax, Martine; University of Oxford, DNA Damage Group, CRUK/MRC Oxford Institute for Radiation Oncology Cadet, Jean; CEA, INAC

SCHOLARONE™
Manuscripts

Cite this: DOI: 10.1039/c0xx00000x

www.rsc.org/xxxxxx

ARTICLE TYPE

Effects of (5'*S*)-5',8-cyclo-2'-deoxyadenosine on the base excision repair of oxidatively generated clustered DNA damage. A biochemical and theoretical study.

Boleslaw T. Karwowski[*a,b], Sophie Bellon[c], Peter O'Neill[c], Martine E. Lomax[c] and Jean Cadet[bd]

Received (in XXX, XXX) XthXXXXXXXXX 20XX, Accepted Xth XXXXXXXXX 20XX
DOI: 10.1039/b000000x

The presence of 5',8-cyclo-2'-deoxyadenosine (5'*S*)-cdA induces modifications in the geometry of the DNA duplex in the 5'-end direction of the strand and in the 3'-end direction for the complementary strand. As a consequence, the enzymes are probably not able to adjust their active sites in this rigid structure. Additionally, clustered DNA damage sites, a signature of ionising radiation, pose a severe challenge to the cell's repair machinery, particularly base excision repair (BER). To date clusters containing a DNA base lesion, (5'*S*)-cdA, which is repaired by nucleotide excision repair, have not been explored. We have therefore investigated whether bistranded clusters containing (5'*S*)-cdA influence the repairabilty of an opposed AP site lesion, which is repaired by BER. Using synthetic oligonucleotides containing a bistranded cluster with (5'*S*)-cdA and an AP site at different interlesion separations, we have shown that in the presence of (5'*S*)-cdA on the 5'-end side, the repair of the AP site by the BER machinery is retarded when the AP site is ≤ 8 bases from the (5'*S*)-cdA. However, if (5'*S*)-cdA is located on the 3'-end side with respect to the AP site, the effect on its repair is much weaker and totally disappears for distances ≥8 bases.

Introduction

By definition, clustered damage sites in DNA consist of ''two or more individual lesions within one or two helical turns of the DNA helix''[1,2] and are thought to be signatures of ionising radiation. These types of lesions are formed in DNA as the result of radiation-induced multiple radical and excitation hits through a singly radiation track event. The oxidatively generated clustered damage to cellular DNA may consist, in addition to double strand breaks, of single strand breaks with base lesions including 8-oxo-7,8-dihydroguanine (8-oxoGua), 5,6-dihydroxy-5,6-dihydrothymine, 5-formyluracil, 5-hydroxymethyluracil and apurinic/apyrimidic (AP) sites[3,4]. In addition tandem lesions such as purine 5',8-cyclo-2'-deoxyribonucleosides[5,6], guanine-thymine intrastrand[7,8] and interstrand cross-links[9] that arise from one hydroxyl radical or one-electron oxidation hit may be also involved in the composition of the radiation-induced formation of clustered DNA damage sites. Most oxidatively generated base DNA lesions are removed via the base excision repair (BER)[10] mechanism due to the action of specific glycosylases which initiate the repair process according to the short (SP) or long patch (LP) pathway. It should be pointed out that the main difference between the two BER pathways deals with the number of newly inserted nucleotides. In the SP scenario only one nucleotide is replaced by the correct one; on the other hand in the LP pathway two or more nucleotides are inserted by enzymes. The details of the two BER pathways are reported in Scheme 1S (supplementary materials). A hierarchy of repair exists for processing non-DSB clustered damage sites whereby an AP site

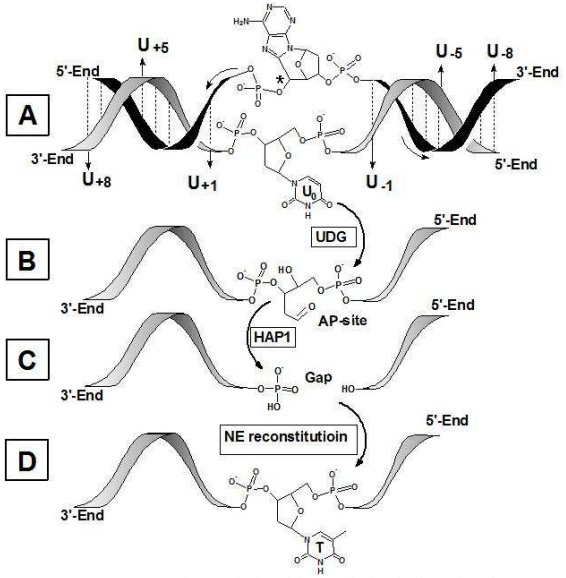

Figure 1. A) Location of the bistranded lesion in the 40-mer oligonucleotides that were investigated, **B**) Abasic site (AP-site) formation upon excision of uracil by uracil DNA *N*-glycosylase (UDG), **C**) Conversion of the abasic site into a single strand break i.e. gap (Gap) followed by **D**) Reconstitution of original strand by nuclear cell extract (NE). The numbers indicated the position of 2'-deoxyuridine (U) relative to (5'*S*)-cdA, U0 opposite to cdA, U-1, U-5, U-8 on the 3'-end of cdA, U+1, U+5, U+8 on the 5'-end of (5'*S*)-cdA.

Table 1. Sequence of oligodeoxynucleotides.

Name		Sequence																																						Position
Con.1	3'	G	A	G	A	A	T	C	G	A	T	C	C	T	T	A	T	A	C	A	**A**	A	G	A	T	A	C	G	A	C	C	C	T	C	G	T	T	T	C	C	G	Control
	5'	C	T	C	T	T	A	T	C	T	A	G	G	A	A	T	A	T	G	T	**U**	T	C	T	A	T	G	C	T	G	G	G	A	T	C	A	A	A	G	G	C	
Con.2	3'	G	A	G	A	A	T	C	G	A	T	C	C	T	T	A	T	A	C	A	**Y**	A	G	A	T	A	C	G	A	C	C	C	T	C	G	T	T	T	C	C	G	Control
	5'	C	T	C	T	T	A	T	C	T	A	G	G	A	A	T	A	T	G	T	T	T	C	T	A	T	G	C	T	G	G	G	A	T	C	A	A	A	G	G	C	
U_0	3'	G	A	G	A	A	T	C	G	A	T	C	C	T	T	A	T	A	C	A	**Y**	A	G	A	T	A	C	G	A	C	C	C	T	C	G	T	T	T	C	C	G	0
	5'	C	T	C	T	T	A	T	C	T	A	G	G	A	A	T	A	T	G	T	**U**	T	C	T	A	T	G	C	T	G	G	G	A	T	C	A	A	A	G	G	C	
U_{-1}	3'	G	A	G	A	A	T	C	G	A	T	C	C	T	T	A	T	A	C	A	**Y**	A	G	A	T	A	C	G	A	C	C	C	T	C	G	T	T	T	C	C	G	-1
	5'	C	T	C	T	T	A	T	C	T	A	G	G	A	A	T	A	T	G	**U**	T	T	C	T	A	T	G	C	T	G	G	G	A	T	C	A	A	A	G	G	C	
U_{-5}	3'	G	A	G	A	A	T	C	G	A	T	C	C	T	T	A	T	A	C	A	**Y**	A	G	A	T	A	C	G	A	C	C	C	T	C	G	T	T	T	C	C	G	-5
	5'	C	T	C	T	T	A	T	C	T	A	G	G	A	A	**U**	A	T	G	T	T	T	C	T	A	T	G	C	T	G	G	G	A	T	C	A	A	A	G	G	C	
U_{+1}	3'	G	A	G	A	A	T	C	G	A	T	C	C	T	T	A	T	A	C	A	**Y**	A	G	A	T	A	C	G	A	C	C	C	T	C	G	T	T	T	C	C	G	+1
	5'	C	T	C	T	T	A	T	C	T	A	G	G	A	A	T	A	T	G	T	T	**U**	C	T	A	T	G	C	T	G	G	G	A	T	C	A	A	A	G	G	C	
U_{+5}	3'	G	A	G	A	A	T	C	G	A	T	C	C	T	T	A	T	A	C	A	**Y**	A	G	A	T	A	C	G	A	C	C	C	T	C	G	T	T	T	C	C	G	+5
	5'	C	T	C	T	T	A	T	C	T	A	G	G	A	A	T	A	T	G	T	T	T	C	T	A	**U**	G	C	T	G	G	G	A	T	C	A	A	A	G	G	C	
U_{-8}	3'	G	A	G	A	A	T	C	G	A	T	C	C	T	T	A	T	A	C	A	A	A	G	**Y**	T	A	C	G	A	C	C	C	T	C	G	T	T	T	C	C	G	-8
	5'	C	T	C	T	T	A	T	C	T	A	G	G	A	A	**U**	A	T	G	T	T	T	C	T	A	T	G	C	T	G	G	G	A	T	C	A	A	A	G	G	C	
U_{+8}	3'	G	A	G	A	A	T	C	G	A	T	C	C	T	T	A	T	**Y**	C	A	A	A	G	A	T	A	C	G	A	C	C	C	T	C	G	T	T	T	C	C	G	+8
	5'	C	T	C	T	T	A	T	C	T	A	G	G	A	A	T	A	T	G	T	T	T	C	T	A	**U**	G	C	T	G	G	G	A	T	C	A	A	A	G	G	C	

Abbreviations: **A** –2'-deoxyadenosine, **Y** – (5'*S*)-5',8-cyclo-2'-deoxyadenosine, **U** – 2'-deoxyuridine, **Name** indicated the acronym of *ds*-oligodeoxynucleotide used in this study: **Con.1** (Control 1) is the control *ds*-oligodeoxynucleotide containing 2'-deoxyuridine as a single lesion, **Con.2** (Control 2) is the control *ds*-oligodeoxynucleotide containing (5'*S*)-5',8-cyclo-2'-deoxyadenosine as a single lesion, **U_0, U_{-1}, U_{-5}, U_{-8}, U_{+1}, U_{+5}, U_{+8}** are the *ds*-oligodeoxynucleotides with both discussed lesions i.e. (5'*S*)-cdA and 2'-deoxyuridine. Numbers indicate the position of U versus (5'*S*)-cdA, as depicted in Figure 1A.

or the SSB resulting from AP site processing retards the excision of a base lesion until the SSB has been repaired.

Using mammalian nuclear or whole cell extracts, it has previously been shown that the repair of an abasic (AP) site or the resulting SSB is reduced when a base lesion is within five bases of the AP site/SSB compared to the efficiency of repair of an AP site/SSB present in isolation. The nature of the base lesion influences the extent of the reduction in repair. For instance 8-oxoGua, thymine glycol, and 5,6-dihydrothymine, base lesions which utilise BER for their repair, results in a 1.2 - 8 fold reduction in the efficiency of the repair of an opposing AP site/SSB and the effect was seen in both the positive and negative orientations (for review see Eccles *et al.*[2b] and Georgakilas *et al.*[2c]). Additionally, the excision of these base modifications does not occur until the AP site/SSB are repaired and as a consequence the lifetime of the cluster is extended. However, DNA damage, such as purine 5',8-cyclo-2'-deoxyribonucleosides[11-13], the tandem base modification between thymine and guanine[14], are removed by the more complicated nucleotide excision repair (NER) pathway[15]. Enzymes involved in the latter repair process recognize and then release the lesion from DNA as part of single stranded oligonucleotide consisting of at least 20-mers[16]. It is important to note that the frequency of lesions in gamma-irradiated cellular DNA decreases with the increase in the linear energy transfer (LET) of radiation while the complexity of the clustered damage increases[17]. The formation of oxidatively generated clustered DNA damage can lead to various cell responses (necrosis, apoptosis, etc.)[18,19], which is significant from a biological/medical point of view.

Several groups have investigated the effect of lesions[20] such as AP, 8-oxo-7,8-dihydroguanine (8-oxoGua)[21,22] and 5,6-dihydroxy-5,6-dihydrothymine[23] in the matrix strand on the repair of an AP site in the opposite strand. In this article, we have therefore investigated whether bistranded clusters containing (5'*S*)-cdA influence the repairability of an opposed AP site lesion, which is repaired by BER, emphasising the delineation of the effects of 5'*S* diastereomer of 5',8-cyclo-2'-deoxyadenosine (cdA) present in one strand of double stranded (*ds*)-DNA on the repair process of an

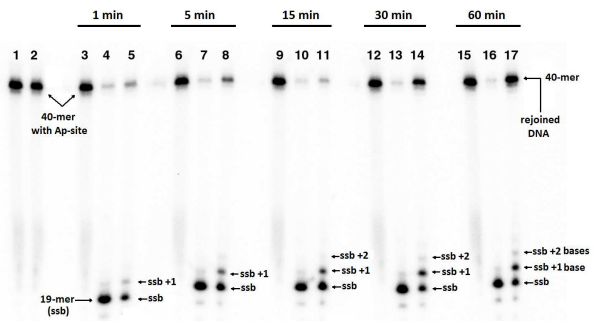

Figure 2. Repair of an AP-site, formed by digestion with UDG to (conversion of 2'-deoxyuridine to abasic site), in Con.1 (40-mer) . Representative gel showing the cleavage and the rejoining of an AP-site in the [^{32}P]-oligodeoxynucleotides and treated with NE in the absence of (5'*S*)-cdA in the complementary strand. Lanes **1** (0 sec), **2** (after 60 min) are the control samples. Lanes **3**, **6**, **9, 12** and **15** are samples containing the [^{32}P]-oligodeoxynucleotide and NE buffer. Lanes **4, 7, 10, 13, 16** containing the [^{32}P]-oligodeoxynucleotides, NE buffer and NE (1.1µl for sample)-the cleavage assay. Lanes **5**, **8**, **11**, **14**, **17** containing the [^{32}P]-oligodeoxynucleotides, NE buffer, dNTP and NE (1.1µl for sample)-the repair assay. SSB – single strand DNA break.

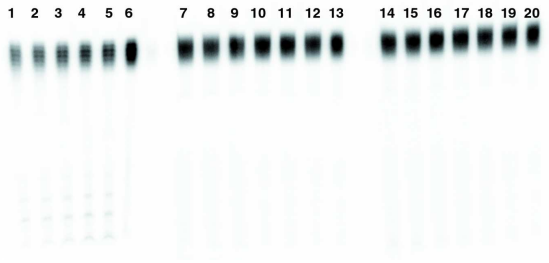

Figure 3.Visualization of Con.2 (40-mer) stability in the presence of Nth, FPG, NE. Lane **1-6,** respectively 0.0; 0.5; 1.0; 2.5; 5.0; 10 µg per sample of nuclear extract from xrs5 cells (NE). Lane **7-13,** respectively 0.0; 1.0; 10.0; 100.0 pg 1.0; 10.0; 100.0 ng per sample of FPG. Lane **14-20,** respectively 0.0; 1.0; 10.0; 100.0 pg 1.0; 10.0; 100.0 ng per sample of Nth.

AP-site introduced on the complementary strand. The bistranded lesions are located at a distance, varying between them from 0 to 8 nucleotide separation Table 1. As (5'*S*)-cdA is not a substrate for the BER machinery[11], a single-strand break (SSB) following processing of the AP-site in nuclear extracts (NE) by BER is formed initially. Figure 1 outlines the general scheme using synthetic 40-mer oligonucleotides containing the clustered damage sites and treatment with NE as originally outlined in reference 20a .

Results and Discussion

The activity of NE, UDG enzymes toward (5'*S*)-cdA containing *ds*-DNA fragments

In the BER machinery the action of different enzymes takes place[10]. The DNA repair process starts from the damage recognition followed by its excision by the DNA glycosylase, from the oligonucleotides. In this study, uracil DNA N-glycosylase (UDG), which recognizes the uracil residue due of A:::U pair instability, was used[24] to form, an AP-site prior to treatment of the 40-mer oligonucleotides with NE for a given times. The activity of UDG and xrs5 cell nuclear extracts (NE) was confirmed by one pot digestion of control 40-mer double stranded oligonucleotide that contained only 2'-deoxyuridine (dU) as the modification (Con.1) – see Table 1. This strategy was chosen due to the similar mobility of the DNA fragment containing the AP-site and the non hydrolyzed fragment. As shown in Figure 2. The strand containing the AP site in Con.1 is almost completely incised after one minute incubation with the NE resulting in appearance of a shorter oligonucleotide, corresponding to the 20-mer, as would be predicted. This result also indicates that the previous treatment of the oligonucleotide with UDG was highly effective. Additionally, any influence of (5'*S*)-cdA on the UDG activity of converting the uracil into AP sites in the clusters was not seen. This is probably due to the fact that the glycosylase interacts only with one strand of *ds*-DNA without strong contacts with the complementary oligodeoxynucleotide[25]. Incubation of Con.1 with NE for longer times also provided confirmation of NE activity, since the intensity of the band corresponding to the reconstituted 40-mer was found to increase with the reaction time in the presence of dNTP. This finding is consistent with previous observations[21]. It has been shown that (5'*S*)-cdA is not a substrate for known glycosylase enzymes, probably due to the presence of an additional C5'-C8 covalent bond, which prevents removal of the lesion from DNA. However the lack of data concerning the resistance of (5'*S*)-cdA to glycosylase hydrolysis in the presence of NE prompted us to undertake an additional stability test. To check the resistance of double stranded oligodeoxynucleotide containing (5'*S*)-cdA towards digestion by NE, formamidopyrimidine DNA *N*-glycosylase (FPG) and endonuclease III (Nth) (at different concentrations) ^{32}P labelled oligodeoxynucleotide contain only (5'*S*)-cdA as modification (Con.2) was incubated at 37°C for 30 min (Figure 3). It was found that Con.2 is stable in the presence of the enzymes – no corresponding 20-mer oligonucleotides were observed, as shown

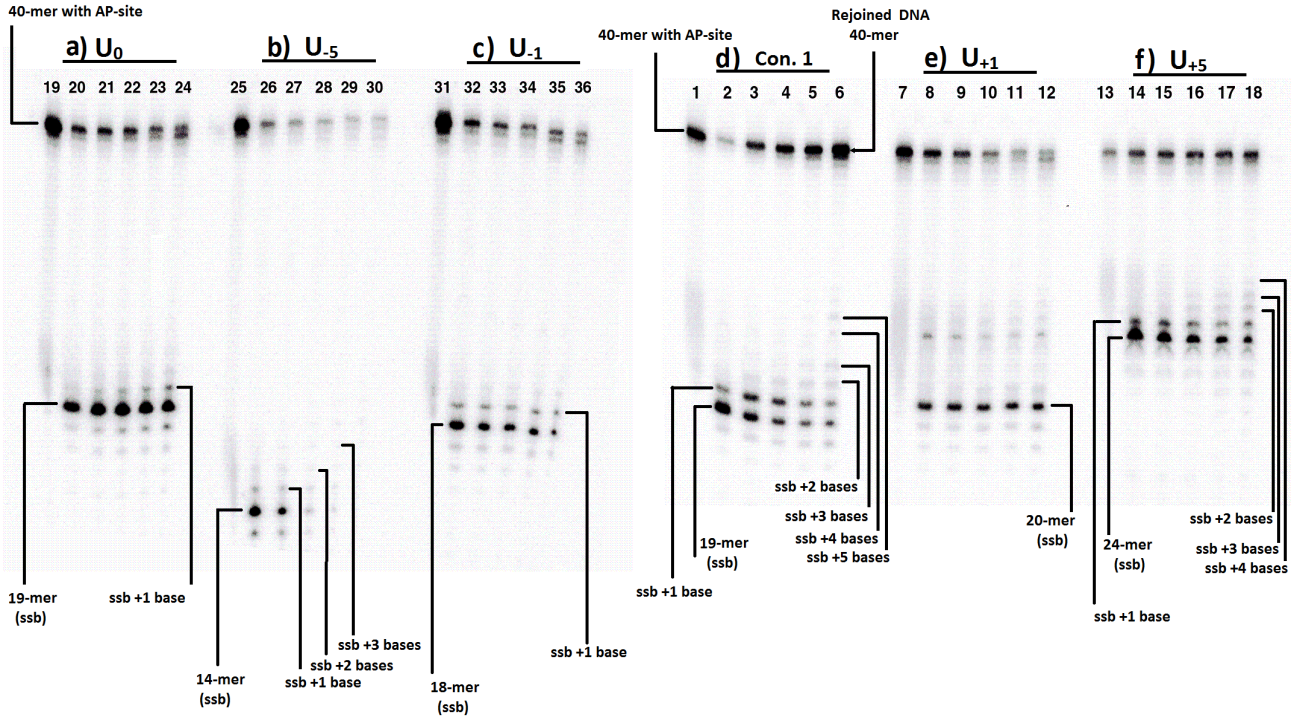

Figure 4. Representative denaturing polyacrylamide gel showing the rejoining of an AP-site in the presence of NE, AP-site formed from *ds*-oligonucleotide namely: U_0, U_{-1}, U_{-5}, U_{+1}, U_{+5} and Cont.1, under UDG activity (Table 1, Figure 1). **a)** Lane 19-24 corresponded to the opposite position of dU versus (5'*S*)-cdA present in construct U_0; **b)** Lane 25-30 corresponded to the distance between dU and dA equal to -5 bases present in construct U_{-5}; **c)** Lane 31-36 corresponded to the distance between dU and (5'*S*)-cdA equal to -1 base present in construct U_{-1}; **d)** Lane 7-12 corresponded to the distance between dU and dA equal to 0 bases present in reference *ds*-oligonucleotide Con.1; **e)** Lane 7-12 corresponded to the distance between dU and dA equal to +1 base present in construct U_{+1}; **f)** Lane 13-18 corresponded to the distance between dU and dA equal to +5 bases present in construct U_{+5}. In all cases the following order of reaction times was used 0, 1, 5, 15, 30, 60 min starting from the left end site.

in Figure 2. However, low level of degradation of *ds*-oligodeoxynucleotide was observed in the case of NE treatment, probably due to the presence of exo- and endonucleases activities as well as some kind of interactions between enzymes (Nth, FPG) and *ds*-DNA has been become as smeared bands, see Figure 3. Therefore, it was concluded that the applied enzymes are active and the oligonucleotide containing (5'*S*)-cdA is stable under the investigated conditions.

Influence of (5'*S*)-5',8-cyclo-2'-deoxyadenosine on the AP-site repair process.

Double-stranded oligodeoxynucleotides, with the specific location of dU versus (5'*S*)-cdA, as shown in Table 1, were chosen to investigate the effects of purine 5',8-cyclo-2'-deoxyribonucleoside on DNA BER repair efficiency of the AP site. All the experiments were carried out using the procedure described in the experimental section. The position of clustered lesions was selected following previous experiments performed by the group[21]. It was shown that the efficiency of enzymes involved in the BER process depended on the relative position of the two selected lesions in the clustered damage. The more pronounced efficiency decrease in the DNA SSB rejoining was observed when the AP-site is located in the +1 position to an opposing lesion.

To investigate the effect of (5'*S*)-cdA on the efficiency of repair on the opposing AP site at different locations by BER enzymes present in NE experiments was performed using 40-mer *ds*-oligonucleotides assigned as U_{-5}, U_{-1}, U_0, U_{+1}, U_{+5} presented in Table 1 and schematically in Figure 1, The *ds*-DNA with only a dU residue (Con.1, Table 1) were used as a reference material. The strand containing the AP site was 5'-^{32}P-labelled. The results are presented in Figures 4..A notable inhibition of up to 40% with respect to Con.1 was seen for SSB formation when the AP site was at positions -1, 0, +1 to the (5'*S*)-cdA following incubation for different times up to 60 min (see Table 1, Figure 1). This time was chosen as at longer times degradation of the oligonucleotides in NE starts to occur. As shown in Figures 2, 3 and 4 [^{32}P]-labelled oligonucleotides that contained an AP-site exhibit different mobility with respect to the non-digested one during PAGE electrophoresis analysis due to the change in molecular size upon excision of the AP site. Moreover changes in migration between oligonucleotide strands that possess two different forms of AP-site i.e. cyclic and open one can be expected[26a]. For each set of experiments, the presence of (5'*S*)-cdA in the opposite non-labelled strand led to differences in the cleavage efficiency, depending on the relative location of the AP-site in the complementary strand; the efficiency was found to decrease in the following order when the AP site was located at -5<+5<0<-1<+1. It is inferred that the presence of (5'*S*)-5',8-cyclo-2'-deoxyadenosine strongly hinders the incision of the AP-site to form a SSB. It is known that the activity of endonuclease HAP-1 requires direct contact between the enzyme and the AP-site in ds-DNA[26b].

The role of the (5'*S*)-cdA effect on the polymerase activity, involved in the BER machinery (Scheme 1S) was also explored. The incorporation of a single base into the SSB was observed when the distance between the selected lesions was at position: –1, 0, +1 (Figure 1 and 4) although bands corresponding to incorporation of 2 or more bases were not noted. Similar results were reported by Kuruoka *et al.* for the Pol-η polymerization reaction in the context of purine 5',8-cyclo-2'-deoxyribonucleoside[11]. The incorporation of one base was still observed when the distance was increased up to +5 bases between the AP-site and (5'*S*)-cdA (Figure 4, Figure 1S, Table 1). Surprisingly, the incorporation of one base appears to be less efficient when the position of the AP site is shifted from +5 to -5 (Figure 4). For some unknown reason, a partial loss of radioactivity was noted for the experiment involving the U-5 DNA strand. The enzymatic reaction were repeated several times but in each case similar results were obtained i.e. a notable loss of ^{32}P radioactivity with the U-5 oligonucleotide, although reconstitution of the expected DNA as an indication of the repair of the AP site/SSB was observed if the AP site/SSB is at position -5 bases (compound U_{-5}) or at +5, as shown in Figures 4 and 1S. The effect of (5'*S*)-cdA on the efficiency of repair of the AP site/SSB is shown graphically in Figure 1S, clearly showing a low level of repair when the two lesions are complementary partners (U0) or when the AP site is at positions -1 or +1. Repair of the AP site occurs when (5'*S*)-cdA is located at positions +5 and -5, although the extent of repair is reduced compared with the control AP site

The above results prompted us to extend the distance between the two lesions up to -8 and +8 bases. Due to the lack of suitable thymidine (toward 3'-end of strand contained (5'*S*)-cdA), which enables its replacement by dU and to gain access to suitable *ds*-oligonucleotides, without sequence changes, the modified DNA fragments namely U_{-8} and U_{+8} were constructed (Table 1) and the repair assay with NE is shown in Figure 5. The control oligodeoxynucleotides that only contain (5'*S*)-cdA were found to be stable in the NE up to 60 min. With the clustered damage

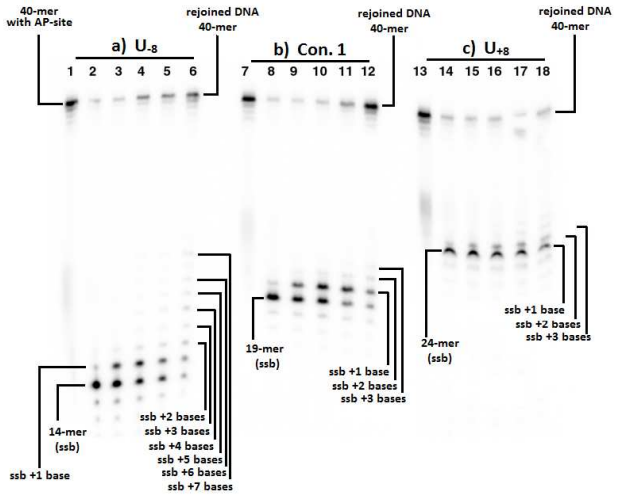

Figure 5. Representative denaturing polyacrylamide gel showing the rejoining of an AP-site in the presence of NE, AP-site formed from *ds*-oligonucleotide: Cont.1, U-8 and U+8 under UDG activity (Table 1, Figure 1). a) Lane 1-6 corresponded to the *ds*-oligo (U_{-8}) in which the distance between dU and (5'*S*)-cdA is equal to -8 bases ; b) Lane 7-12 corresponded to the *ds*-oligo (Con. 1) in which the distance between dU and dA is equal to 0 base; c) Lane 13-18 corresponded to the *ds*-oligo (U_{+8}) in which the distance between dU and (5'*S*)-cdA is equal to +8 bases. In all cases the following order of reaction times was used 0, 1, 5, 15, 30, 60 min. starting from the left site.

sites, when the AP site/SSB is 8 bases to the (5'*S*)-cdA, U_{+8}, a decrease in the polymerase activity seen as the incorporation of bases and low levels of repair of the AP site/SSB were observed (Figure 1 and Figure 5: Lanes 14-18). Conversely, when the AP site/SSB is located 8 bases to (5'*S*)-cdA in U-8 the polymerase activities on the studied and control, Con.1, are comparable, and repair of the AP site/SSB by the BER machinery was also observed (see Figure 5, Lane 2-6).

It is important to mention here that the presence of more than one band, representing 2 or more bases incorporated, arising from the polymerase activity in Figures 2, 4 and 5 is indicative of the involvement of the long patch BER pathway. This is particularly apparent for experiments with (5'*S*)-cdA containing *ds*-oligonucleotides.

Theoretical Study

The explanation of the above phenomena – the influence of (5'*S*)-cdA on the *ds*-DNA three dimensional structure that contained (5'*S*)-cdA in one strand and dU, AP-site or *ss*-DNA break in the complementary strand – was inferred from molecular mechanics investigations (details given in the experimental part) using the Amber94 force field in the solvation box. Table 2 presents the nucleobase sequence of *ds*-DNA models. Thus 18 *ds*-oligonucleotides (13-mers) were used in this study. Due to the complexity of the system, only the central part, the most stable one, of the duplex was chosen for further spatial geometry optimization and subsequent theoretical consideration (indicated in Table 1 as a shaded part). It is worth mentioning here that 9 of investigated duplexes represented the native form of *ds*-DNA, the remaining 9 duplexes are considered as clustered damaged oligonucleotides. Due to the fact that both subunits in the purine 5',8-cyclo-2'-deoxyribonucleoside structure have been modified

Table 2. The central part of DNA duplexes optimized by the Molecular Mechanics approach is in Table 1, as shaded boxes.

Name	Oligonucleotide sequence													
Matrix - 1	**3'-end**	^{13}C	^{12}A	^{11}T	^{10}A	^{9}G	^{8}A	^{7}**A**	^{6}A	^{5}C	^{4}A	^{3}T	^{2}A	^{1}T	**5'-end**
dA(U0)		G_1	T_2	A_3	T_4	C_5	T_6	**U_7**	T_8	G_9	T_{10}	A_{11}	T_{12}	A_{13}	
dA(Ap0)		G	T	A	T	C	T	**AP**	T	G	T	A	T	A	
dA(Ga0)		G	T	A	T	C	T	---	T	G	T	A	T	A	
dA(U-1)		G	T	A	T	C	**U**	T	T	G	T	A	T	A	
dA(Ap-1)	**5'-end**	G	T	A	T	C	**AP**	T	T	G	T	A	T	A	**3'-end**
dA(Ga-1)		G	T	A	T	C	---	T	T	G	T	A	T	A	
dA(U+1)		G	T	A	T	C	T	T	**U**	G	T	A	T	A	
dA(Ap+1)		G	T	A	T	C	T	T	**AP**	G	T	A	T	A	
dA(Ga+1)		G	T	A	T	C	T	T	---	G	T	A	T	A	
	Oligonucleotide sequence consist tandem lesioin (5'*S*)-cdA														
Matrix - 2	**3'-end**	^{13}C	^{12}A	^{11}T	^{10}A	^{9}G	^{8}A	^{7}**Y**	^{6}A	^{5}C	^{4}A	^{3}T	^{2}A	^{1}T	**5'-end**
cdA(U0)		G_1	T_2	A_3	T_4	C_5	T_6	**U_7**	T_8	G_9	T_{10}	A_{11}	T_{12}	A_{13}	
cdA (Ap0)		G	T	A	T	C	T	**AP**	T	G	T	A	T	A	
cdA(Ga0)		G	T	A	T	C	T	---	T	G	T	A	T	A	
cdA(U-1)		G	T	A	T	C	**U**	T	T	G	T	A	T	A	
cdA(Ap-1)	**5'-end**	G	T	A	T	C	**AP**	T	T	G	T	A	T	A	**3'-end**
cdA(Ga-1)		G	T	A	T	C	---	T	T	G	T	A	T	A	
cdA(U+1)		G	T	A	T	C	T	T	**U**	G	T	A	T	A	
cdA(Ap+1)		G	T	A	T	C	T	T	**AP**	G	T	A	T	A	
cdA(Ga+1)		G	T	A	T	C	T	T	---	G	T	A	T	A	

A – represents 2'-deoxyadenosine , **Y** – represents (5'*S*)-5',8-cyclo-2'-deoxyadenosine, **U**– 2'-deoxyuridine, **AP**–apurinic/apyrimidinic site (abasic site, AP-site), as a result of dU conversion to AP-site, --- – single strand DNA break i.e. gap, formed after **AP-site** excision. **Matrix -1** – is a complementary strand, to the strands denoted as follow: dA(U0), dA(Ap0), dA(Ga0), dA(U-1), dA(Ap-1), dA(Ga-1), dA(U+1), dA(Ap+1), dA(Ga+1). **Matrix -2** – is a complementary strand, with (5'*S*)-cdA as the lesion, to the strands denoted as follow: cdA(U0), cdA(Ap0), cdA(Ga0), cdA(U-1), cdA(Ap-1), cdA(Ga-1), cdA(U+1), cdA(Ap+1), cdA(Ga+1). Numbers in superscript and subscript indicated the order of nucleobases in the double helix strands.

i.e. 2-deoxyribose and adenine, (5'*S*)-cdA, by definition, is a tandem DNA lesion. To deduce the influence of (5'*S*)-cdA on the spatial geometry of *ds*-DNA the standard reference frame strategy descripted by Olson *et al.* was used[27]. The conformational analysis of three-dimensional nucleic acid structures was achieved by considering the following parameters: local base pairs, base pairing, helix length and bend. The helix bend parameter was assigned following the Fujimoto strategy[28]. Moreover due to the flexibility of DNA sugar-phosphate backbone, the suitable dihedral angles and 2-deoxyribose puckering were taken into consideration. The conformation data for all discussed 18 *ds*-oligonucleotides are given in the supplementary material (these include the graphical representation of DNA duplexes and the schematic representation of discussed parameters). Figure 2S provides graphical representations of each of the disused duplexes (see Table 2).

The average values of structural parameters (complementary base, base pairing, local helical) between unmodified/modified *ds*-DNA corresponding pairs i.e: dA(U0)/cdA(U0), dA(Ap0)/cdA(Ap0), dA(Ga0)/cdA(Ga0), dA(U-1)/cdA(U-1), dA(Ap-1)/cdA(U-1), dA(Ga-1)/cdA(Ga-1),dA(U+1)/cdA(U+1), A(Ap+1)/cdA(Ap+1), dA(Ga+1)/cdA(Ga+1) are reported in Table 1S and graphically represented in Graph 1S.

This analysis indicates that the presence of (5'*S*)-cdA in *ds*-DNA does not change significantly the structural parameters if 2'-deoxyuridine is present in the complementary strand. The conversion of dU to corresponding AP-site allowed the helix to adopt the energetically favored conformation in the vicinity of the rigid purine 5',8-cyclo-2'-deoxyribonucleoside – as the likely result of helix relaxation. This situation was noticeable for *ds*-oligodeoxynucleotides in which the abasic site was shifted to the 5'-end direction of the strand with (5'*S*)-cdA (AP-site was present in complementary strand at position T8) (Table 2, Figure 1). The following local helix parameters: stagger, propeller, helix length and bend have been founded as the most sensitive ones. The generation of the SSB (gap) in place of suitable AP-site abolishes the helix tension, induced by the presence of (5'*S*)-cdA. The analyses of above mentioned four parameters have shown the same trends, as was previously found for *ds*-DNA fragments which possess both lesions: AP-site and (5'*S*)-cdA. Only in the case of *ds*-oligonucleotide cdA(Ga+1) the shortening by 0.39Å of helix length was observed in comparison with dA(Ga+1) which retains the helix bend value to a similar extent (142.33^o and 142.99^o respectively). Further analysis of base pair parameters (Table 1S, Graph 1S) disclosed the notable differences in the case of stretch, buckle and opening for the following *ds*-oligonucleotide pairs comparison dA(U0)/cdA(U0), dA(U-1)/cdA(U-1),dA(U-1)/cdA(U-1). Changes in the buckle parameter were noted mainly at position ^{7}A corresponding to (5'*S*)-cdA i.e. 1.67/-17.46, 4.44/-19.2, -14.63/-5.16 respectively to dA(U0)/cdA(U0), dA(U-1)/cdA(U-1),dA(U+1)/cdA(U+1). Surprisingly for the pair dA(U0)/cdA(U0) the opening parameter has shown ~16^o differences for the base pair marked as ^{8}A::T_6, for other two *ds*-DNA pairs these differences were minimal. The analysis of base pair step parameters i.e. rise and twist (Table 2S, Graph 2S) have shown to increase in all investigated *ds*-DNAs. The discussed *ds*-oligodeoxynucleotides contained the 5',8-cyclo-2'-deoxyribonucleoside in their central part is composed of the

following base pairs ^{6}A::T$_8$, ^{7}cdA::T$_7$ and ^{8}A::T$_6$ (in comparison with native duplexes, in which the central part is composed as follow ^{6}A::T$_8$, ^{7}A::T$_7$ and ^{8}A::T$_6$). The presence of (5'*S*)-cdA led to increases in the value of the "rise - base pairs dimer parameter" by 0.38Å, 0.54Å, 0.43Å and twist by 16°, 14°, 7° for dA(U0)/cdA(U0), dA(U-1)/cdA(U-1), dA(U+1)/cdA(U+1) *ds*-DNA pairs respectively. Similar observations were made for local helical parameters i.e. h-rise and h-twist (Table 2S and Graph 2S). The following differences values were found for dA(U0)/cdA(U0), dA(U-1)/cdA(U-1), dA(U+1)/cdA(U+1) *ds*-DNA pairs 0.3Å/17°, 0.53Å/14°, 0.49Å/7° h-rise/h-twist respectively.

The presence of an AP-site in place of dU allowed helix to relax at the position of (5'*S*)-cdA. This is inferred from the reduction of the differences in the base pair step and local helical parameters values between clustered damage *ds*-DNA and *ds*-oligonucleotides which possess only single lesion – AP-site, see Table 3S and Graphs 3S. The purine 5',8-cyclo-2'-deoxyribonucleoside, when present as the complementary base to thymidine still affects base pair parameters, The differences in buckle and opening parameters were found as follow: 21.2°/27.4° and 5.6° /10° for dA(Ap-1)/cdA(Ap-1), dA(Ap+1)/cdA(Ap+1) respectively.

The subsequent processing of apurinic/apyrimidinic site gives rise to SSB in the *ds*-DNA structure. In this case, as expected, (5'*S*)-cdA has a disturbing effect on the structure of *ds*-oligonucleotide, however only at the site of its formation. Therefore, the remaining part of double helix in 3'-end and 5'-end directions (relatively to purine 2'-deoxyribonucleoside) can adopt the most energetically privileged structure, as in native *ds*-DNA (Table 4S, Graphs 4S). Therefore, only changes in base pair parameters corresponding to the pair formed by (5'*S*)-cdA and thymidine, denoted as ^{7}A::T$_7$ were observed. This is particularly true for the opening parameter, which shows the following values: 8.1° and 10.0° for cdA(Ga-1) and cdA(Ga+1) respectively instead of -3.5° and -4.2° found for dA(Ga-1) and dA(Ga-1).

The presence of (5'*S*)-cdA leads to modifications in the hydrogen bond (HB) length (Table 5S, Graph 5S) as already noted for structural parameters of the sugar-phosphate backbone. If the clustered lesion containing *ds*-DNA fragments can be considered as continuous structures (cdA(U0), cdA(U-1), cdA(U+1)) the presence of (5'*S*)-cdA induces changes of HB length in its close vicinity. The following values were found: for HB2 present in ^{8}A::T$_6$ base pair: 2.88Å/3.4Å and 2.88Å/3.08Å for dA(U0)/cdA(U0) and dA(U-1)/cdA(U-1) respectively. For the *ds*-oligodeoxynucleotide dA(U+1)/cdA(U+1) these values were found as follow: 2.97Å/3.12Å. Similar trends were observed for *ds*-oligodeoxynucleotides that contain an AP-site as shown in Table 5S. The formation of the SSB leads to helix structure relaxation, with remaining disturbing effects of (5'*S*)-cdA, at position ^{7}A, only however when paired with thymine T$_7$. The highest differences in hydrogen bond length have been found for HB1of^{7}A::T$_7$ base pair in the DNA duplexes denoted as dA(Ga+1) and cdA(Ga+1) respectively: 2.88Å and 3.46Å.

Based on above results, we finally have taken the following parameters into consideration for base pairs: λ(I), λ(2), D1, D2, L and for base pair step: minor and major groove width (data reported in Table 6S and Graphs 6S). The analysis shows that the presence of the purine 5',8-cyclo-2'-deoxyribonucleoside induces changes in base pair parameters at the site of its location. It has been manifested by the major groove width increases. Surprisingly only for oligodeoxynucleotides in which (5'*S*)-cdA is opposite to dU, narrowing of the minor groove was observed (minor groove width: 12.6Å/11.0Å for cdA(U0)/cdA(U0) respectively). As it has been shown, in the graphical representation of the data reported in Table 6S, the formation of the AP-site and subsequently of the SSB almost completely abolished the influence of (5'*S*)-cdA on the above discussed parameters. This was expected due to the helix flexibility that is likely to cause a structural change compensation.

Support for the flexibility of the double helix is provided by sugar-phosphate backbone dihedral angle and 2-deoxyribose pseudorotation phase analysis (Table 7S and Graph 7S). Only the dihedral angles chi (O4',C1',N9,C4) and gamma (C3',C4',C5',O5')

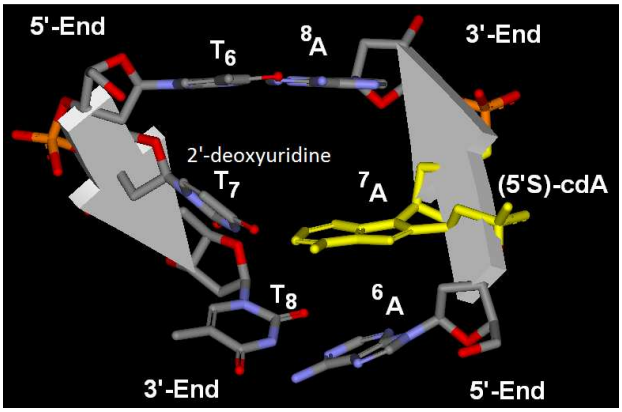

Figure 6. Graphical representation of short double stranded oligonucleotide d[A$_{PO}$(5'*S*)-cdA$_{PO}$A][T$_{PO}$U$_{PO}$T] structure optimised at B3LYP/3-21G** level of theory in gaseous phase.

Table 3. The geometrical parameters of short double stranded oligonucleotide: d[A$_{PO}$(5'S)-dA$_{PO}$A]*[T$_{PO}$dU$_{PO}$T]. Spatial structure optimized at B3LYP/3-21G** level of theory in gaseous phase.

d[AcdAA][TUT]								
Base Pair		λ(1) [°]	λ(2) [°]	D1 [Å]	D2 [Å]	L [Å]	HB1 [Å]	HB2 [Å]
5'	3'							
^{6}A	T$_8$	58.7	55.1	10.2	8.6	9.3	2.63	2.64
^{7}A	U$_7$	56.3	61.9	10.0	8.4	9.3	2.67	2.60
^{8}A	T$_6$	50.3	52.7	10.8	8.9	9.8	2.61	2.59
Base Pair Ideal Model[27]								
A	T	54.5	54.5	10.7			3.05	2.96
A	U	54.6	54.5	10.7			3.02	2.95
Sugar-phosphate backbone parameters								
Base	α	β	γ	δ	ε	ζ	χ	P
^{6}A			77.4	150.0	-162.5	-85.2	-113.1	171.7
^{7}A	-43.2	-87.3	-47.7	146.4	176.6	-43.1	-150.9	265.8
^{8}A	-92.6	-172.3	64.4	84.8			-139.6	4.9
T$_8$	-13.5	-161.9	-32.4	80.7			-113.3	16.2
T$_7$	-57.2	-175.7	57.9	147.3	-159.1	-109.1	-148.6	156.0
T$_6$			56.4	151.6	-173.1	-86.2	-128.6	176.8
Complementary local base pair parameters								
BASE PAIR								
5'-End	3'-End	Share	Stretch	Stagger	Buckle	Propeller	Opening	
^{6}A	T$_8$	0.05	-0.02	0.5	43.11	1.71	-5.85	
^{7}A	U$_7$	-0.23	0.02	0.72	46.42	15.29	0.25	
^{8}A	T$_6$	-0.16	-0.29	-0.08	-3.54	5	-3.83	
DNA B-Form[28b]		0.00	0.15	0.09	0.5	-11.4	0.6	
Local base pairs step parameters								
STEP								
		Shift	Slide	Rise	Tilt	Roll	Twist	
^{6}AA/UT$_8$		0.74	-1.36	4.62	-15.28	-26.95	47.23	
A^{8}A/T$_6$TU		0.32	-1.27	6.86	14.05	-10.85	27.36	
DNA B-Form[28b]		-0.02	0.23	3.32	-0.10	0.6	36	
Local base pair helical parameters								
STEP								
		x-displacement	y-displacement	h-Rise	Inclination	Tip	h-Twist	
^{6}AA/UT$_8$		0.89	-2.12	4.37	-30.17	17.1	56.00	
A^{8}A/T$_6$TU		1.92	4.84	6.35	-20.43	-26.47	32.52	
DNA B-Form[28b]		0.05	0.02	3.29	2.10	0.00	36.5	

assigned for the (5'*S*)-cdA are indicators of stability. Others angles i.e.: alpha, beta, delta, epsilon and zeta show some variability. Moreover, (5'*S*)-cdA forces the strand rigidity in the section/neighborhood next to the lesion position in the oligodeoxynucleotides. This received support by taking into account the graphical representation of the data included in Table 7S. The shapes of the curves, represented the gamma and chi dihedral angles, are similar at each point of the studies and do not depend on the presence of the lesion inserted on the opposite strand, i.e.: 2'-deoxyuridine. The pseudorotation phase values of the sugar ring of 2'-deoxyadenosine units at positions ^{6}A and ^{8}A as well as for (5'*S*)-cdA at position ^{7}A reveal invariability of their value for all investigated *ds*-oligodeoxynucleotides possessing the purine 5',8-cyclo-2'-deoxyribonucleoside (cdA(U0), cdA(Ap0), cdA(Ga0), cdA(U-1), cdA(U-1), cdA(Ga-1), cdA(U+1), cdA(Ap+1), cdA(Ga+1).

Additionally, similar sets of analysis were carried out for control *ds*-DNAs that do not exhibit (5'*S*)-cdA (see Table 7S).

It was found that both strands of the DNA double-helix are highly flexible within the lesion's region. This is due to the fact that the matrix strand can adopt the required spatial geometry, which is constrained by the lesions located on the complementary strand.

Finally, considering the results obtained using enzymatic experiments and Molecular Mechanics calculations, a simple DFT geometry optimization was performed.

For this study the short duplex d[A_{PO}(5'*S*)cdA_{PO}A]*[T_{PO}dU_{PO}T] was selected. For the geometry optimization, the DFT method was used with the B3LYP functional and the small basis set 3-21g**, and the calculation was performed in the gaseous phase. The gaseous phase was chosen due to the fact that in the active site of polymerase β (Polβ) only a few water molecules are present. This scanty amount of additional hydrogen bond leads to an increase in the fidelity of polymerase activity which is crucial for correct replication or more efficient DNA repair process. Secondly the criteria of calculations were chosen taking into consideration the complexity of the system and the necessity of minimizing CPU time consumption. As presented in Figure 6, the presence of (5'*S*)-cdA induces changes in the base pairing geometry according to a "*domino effect*", which extends to the 5'-end direction; surprisingly, no changes were observed in the 3'-end direction. The noted deformation of the base pairing geometry was induced by the rigid structure of (5'*S*)-cdA and the lack of the methyl group in the 2'-deoxyuridine moiety (in comparsion with thymidine). The lack of the latest one, allowed the (5'*S*)-cdA::dU base pair to adopt a favorable spatial geometry/conformation. Contrary to that the presence of methyl group at thymidine moiety, in (5'*S*)-cdA::dT system, reduced the flexibility of formed base pair in *ds*-DNA, due to the neighbor base pairs interaction with mentioned C5 methyl group. Therefore, the external spatial geometry of the *ds*-DNA was slightly distorted. In contrast to that, the internal double helix properties related to the stacking and strength of the hydrogen bond should be significantly different that found in the native one. As shown in Table 3 the significant differences from ideal model of base pair model were noted for (5'*S*)-cdA::dU (position ^{7}A::U_{7}). The following values for (5'*S*)-cdA::dU/dA::dU were respectively found: λ(1) 56.3^{o}/54.6^{o}; λ(2) 61.9^{o}/54.5^{o}; D1 10.0Å/10.7Å; HB1 2.67Å/3.05Å and HB2 2.60 Å /2.95Å. Moreover the dihedral angles: gamma (-47.7^{o}) and chi (-150.9) show approximatively the same values as in the molecular mechanics studies -68.4^{o} and 158.7^{o} for (5'*S*)-cdA respectively. The influence of the purine 5',8-cyclo-2'-deoxyribonucleoside on the double helix spatial geometry has been distinctly disclosed by considering the values of buckle, propeller and opening base pairs parameters which are significantly different from values found for B-DNA (Table 3). Moreover the increases of the buckle parameter were observed for base pair connected to the 5'-end of the purine 5',8-cyclo-2'-deoxyribonucleoside. Additionally the four local base pair parameters: rise, tilt, roll and twist show their highest deviation from their value determined for native B-DNA in 5'-end direction of (5'S)-cdA (Table 3). It should be pointed out that the base pair parameter: rise (6.86 Å) was found to be two–fold higher than for the reference one (3.32Å). A similar observation was noted for the local base pair helical parameters as shown in Table 3. Probably due to the facts mentioned above, that the enzymes involved in the BER machinery showed reduced activity in the 5'-end direction of (5'*S*)-cdA containing strand. Therefore these theoretical results are in good agreement with the biochemical data presented above and previous theoretical studies[29].

Conclusions

It was unequivocally showed that the presence of (5'*S*)-cdA exerts a pronounced influence on the 3D structure of *ds*-DNA. Molecular Mechanics calculations indicate a high geometry stability of the χ and γ dihedral angles in the nucleosides nearest to (5'*S*)-cdA on the same strand. This effect is not altered by the presence of lesions on the complementary strand such as 2'-deoxyuridine, AP-site or SSB. Similarly, the flexibility of the complementary strand seems to be independent on the presence of (5'*S*)-cdA. The conformational analysis, based on standard reference frame descriptors of DNA spatial geometry, has clearly shown the influence of purine 5',8-cyclo-2'-deoxyribonucleoside in the double helixes, mainly when both strands of complementary oligodeoxynucleotides are linear/unbroken i.e. without SSB or AP-sites. Otherwise the flexibility of the sugar-phosphate backbone and the spatial orientation of base pairs can lead to the suppression of spatial disturbing effects of purine 5',8-cyclo-2'-deoxyribonucleoside. This was particularly shown in the case of SSB. It may be inferred from the quantum mechanics study that the presence of (5'*S*)-cdA provokes a "*domino effect*" extending to the 5'-end direction of the strand. The buckle base pair parameter can be recognized as an indicator of the level of "*domino effect*". No domino effect is observed in the 3'-end direction of strand with (5'*S*)-cdA.

The discussed effects are important from a biological point of view because enzymes (polymerases, ligase) involved in the BER machinery exhibit activity on the 3'-end. The presence of (5'*S*)-cdA induces modifications in the geometry of the DNA duplex in the 5'-end direction of the strand and in the 3'-end direction for the complementary strand. For this reason the enzymes are probably not able to adjust their active sites in this rigid structure. Finally, the obtained biochemical results indicate that the presence of (5'*S*)-cdA in the complementary strand on the 5'-end side with respect to the repaired lesion in the opposite is the critical factor for the inhibition of the BER machinery. In the 5'-

end direction, this effect is observed up to 8 bases (the distance between the (5'*S*)-cdA and the repaired lesion). However, if (5'*S*)-cdA is located in the 3'-end side with respect to the AP site/SSB being repaired, the effect is much weaker and is not seen for distances ≥8 bases in the 3'-end direction.

Experimental

Biological Study

Substrate Oligonucleotides

The (5'*S*)-5',8-cyclo-2'-deoxyadenosine and phosphoramidite derivative were obtained by a method described by Cadet et al[11].The 40mer oligonucleotides that contained (5'*S*)-cdA were synthesized via solid-phase synthesis on the 1 mmol scale using a classical phosphoramidite strategy with a slight modification as reported by Brooks et al[11,30]**.** Oligodeoxynucleotides were purified by electrophoresis (20% acrylamide with 7M urea). The 40mer oligonucleotides containing 2'-deoxyuridine (dU) were purchased as HPLC-purified compounds from Genosys. The sequences of the double-stranded oligodeoxynucleotides are presented in Table 1. dU was located at variable positions (position U) opposite to (5'*S*)-cdA residue at a fixed position (position Y) on the complementary strand. In controls **1** and **2** the oligonucleotides exhibit one single lesion that is located on one of the two strands. The nomenclature of the relative positions of the two lesions in the clustered DNA damage site was proposed by David-Cordonnier *et al.*[20a]. A positive or negative number was assigned to each residue in the oligonucleotide. This number refers as to the separation, in base pairs, of one lesion on one strand with Y located 5' (a positive number) or 3' (a negative number) opposite to the lesion on the strand with U.

Preparation of 5′-End-Labeled Oligonucleotides[21]

The 40mer oligonucleotide(0.2 μg) was 5'-end-labeled using 10 units of T4 polynucleotide kinase (Invitrogen, Paisley, U.K.) with 25 μCi of [γ-^{32}P]ATP (6000 Ci/mmol, 10 mCi/mL, Perkin-Elmer) in 20 μL of buffer [70 mMTris-HCl (pH 7.6), 10 mM $MgCl_2$, 100 mM KCl, and 1 mM β-2-mercaptoethanol] for 30 min at 37 °C. Subsequent to purification on a 12% denaturing polyacrylamide gel, the labeled oligonucleotide was hybridized with a 2-fold excess of the purified non radiolabelled complementary strand. Efficient annealing of the oligodeoxynucleotides was checked by electrophoresis using a 12% native polyacrylamide gel.

Preparation of an AP-Site[21]

The purified double-stranded oligodeoxynucleotides that contained a uracil (Ura) residue(s) were treated with 1 unit of uracil DNA *N*-glyscosylase (UDG) (Invitrogen) in 100 μL of buffer [10 mM Tris-HCl (pH 7.5), 50 mM NaCl, and 1 mM EDTA] for 30 min at 37 °C to produce an AP-site. The AP-site-containing oligonucleotides were used immediately after their preparation for repair studies.

Preparation of Nuclear Extracts (NE)[21]

The nuclear extracts were prepared as previously described[31] from Ku80 deficient xrs5 cells[32] in order to avoid possible interference with Ku binding to the termini of linear DNA[33] and SSB[34]**.** Briefly, the cells were harvested in exponential phase, and the pelleted cells were re-suspended in an equal volume of buffer [10 mM HEPES (pH 7.9), 100 mM KCl, 1.5 mM MgCl2, and 0.5 mM DTT] and incubated on ice for 15 min. The cells were lysed by drawing the cell suspension into a 0.5 μm diameter needle 10 times, and the nuclei were collected by a brief centrifugation at 12000g and 4 °C. The nuclear proteins were extracted by incubation in 2/3 volumes of high-salt buffer [20 mM HEPES (pH 7.9), 420 mM NaCl, 25% glycerol, 1.5 mM MgCl2, 0.2 mM EDTA, 0.5 mM DTT, and 0.5 mM PMSF] for 30 min under agitation on ice. Following centrifugation for 10 min at 12000g and 4 °C, the supernatant was dialyzed twice over a total period of 16 h against 1 L of buffer [20 mM HEPES (pH 7.9), 100 mM KCl, 0.2 mM EDTA, 20% glycerol, 0.5 mM DTT, and 0.5 mM PMSF]. The protein concentration that was determined using the Bradford colorimetric technique was found to be comprised between 9.5 and 13.3 mg/mL. Aliquots of nuclear extracts were stored at -80 °C.

Repair Assays[21]

The *ds*-oligodeoxynucleotides (10 000 cpm, 2 fmol) were incubated with either 1 μg (for analysis of the AP-site-containing strand) or 5 μg (for analysis of the 8-oxoGua-containing strand) of xrs5 nuclear extracts in 5 μL of repair buffer [70 mM Tris-HCl (pH 7.5), 10 mM $MgCl_2$, 10 mM DTT, 4 mM ATP, 40 mM phosphocreatine, 1.6 μg/mL phosphocreatine kinase together with dATP, dCTP, dGTP, and dTTP (0.1 mM each)] at 37°C for 0, 1, 5, 15, 30, and 60 min. The efficiency of the AP endonuclease present in the nuclear extract is such that a few s at room temperature is sufficient for most of the AP-site contained in the oligonucleotide to be incised. The concentrations of extract were optimized from titration studies. To stop the reactions, 5 μL of denaturing stop solution (98% formamide, 2 mM EDTA, 0.025% bromophenol blue, and 0.025% xylene cyanol) was added. The samples were then subjected to electrophoresis on a 20% denaturing polyacrylamide gel containing 8 M urea in 1xTBE [89 mM Tris-HCl, 89 mM boric acid, and 2 mM EDTA (pH 8.3)] for 90 min at a constant power of 85 W. The dried gel was exposed to a Bio-Rad PhosphorImager screen for visualization of repair products using the phosphorimaging technology (Molecular Imager FX, Bio-Rad,Hercules, CA) and quantified with the Quantity One software (Bio-Rad, Hercules, CA)[34]. For the time dependence study of the repair of the AP-site, the intensity of the bands representing either single-stranded DNA, *ss*-DNA with one, two, or five added bases, or rejoined DNA [ligation of the AP-site following addition of the missing base(s)] was expressed as the percentage of the total intensities for all bands within each lane, to overcome any differences in loading or in ^{32}P-labelling efficiency. The efficiency of repair of an AP-site within clustered damage sites was compared with that of the respective single AP site in control oligonucleotides. It was found that the different preparations of the xrs5 nuclear extract showed slightly different activities for the repair of an AP-site. To account for this lack of reproducibility, the relative amount of rejoining of an AP-site within a clustered damage site was always compared with that of a control oligodeoxynucleotide containing an AP-site as a single lesion, using the same extract preparation within each experiment.

Theoretical Study

Molecular Mechanics calculation (general procedure)

The 18 different *ds*-oligodeoxynucleotides (13-mers), presented in Table 2, were prepared using the nucleoside database implemented in HYPERHEM 8.0.6 software package[35]. As a starting point for calculation the native 13-mer were chosen in which the methyl group of thymidine in position T7, was replaced by a proton giving the required 2'-deoxyuridine, denoted in Table 2 as oligonucleotide dA(U0). A similar strategy was used for the remaining oligodeoxynucleotides which possess 2'-deoxyuridine in suitable locations (Table 2). The strand, shown in Table 2 as Matrix-2 (possesses 5',8-cyclo-2'-deoxyadenosine, at position 7A) that was derived from native oligonucleotide i.e. Matrix-1 in which 2'-deoxyadenosine, at position 7A, was converted to the C5'-C8 cyclic form i.e. (5'*S*)-cdA. The suitable apurinic/apyrimidinic sites (abasic site, AP-site) were prepared, by remaining suitable atoms from 2'-deoxyuridine. After the base atoms were removed the adequate AP-site was formed in its open form (Figure 1B). The generated abasic site was transformed into the single strand DNA break as shown on Figure 1. The 3'-phosphate group and the remains of pentose moiety have been removed. The missing valences were filled by proton (Figure 1C). The following eighteen *ds*-oligodeoxynucleotides in DNA B-form reported in Table 2 were subjected to molecular mechanics calculations (nine "native" and nine clustered DNA lesions). The following order of the optimization steps in each case was used e.g.: *ds*-DNA with 2'-deoxyuuridine (dA(U0)) →*ds*-DNA with AP-site (dA(Ap0)) →*ds*-DNA with single strand break (dA(Ga0)). For all oligodeoxynucleotides presented in Table 2, calculations were performed in the periodic box of water molecules. The dimension of periodic box was as follows: 35/35/55Å length/width/height, contains 1914 water molecules. To neutralize the negative charge of phosphate groups in both strands, of discussed molecules (Table 2), the Na^+ counterions were placed at a distance of ~4 Å from the phosphorus atom. The Molecular Mechanics optimization was performed at constant temperature 273K. For each system, the optimization process was performed under Molecular Mechanics with: force file Amber94[36], algorithm Polak-Ribière conjugate gradient[37], RMS gradient of: 0.01kcal/(Åmol). The potential energy function was calculated based on contribution from bonds, angles, torsion angles, non-bonded, electrostatic and hydrogen bond functions.

The visualization of all the structures, as well as the creation of suitable *.pdb files was performed using *DS Visualizer* software[38]. The three-dimensional structural analyses of mentioned *ds*-DNAs, based on a standard reference frame, were obtained by the 3DNA software package using the web-based interface w3DNA (web 3DNA)[39].

Quantum mechanics calculations

The spatial molecular structure of short *ds*-DNA fragment $d[A_{PO}(5'S)\text{-}dA_{PO}A]*[T_{PO}dU_{PO}T]$, as a central part of oligodeoxynucleotides reported in Table 2, was optimized. Calculations were performed by the density functional theory (DFT) using the generalized gradient approximation (GGA) exchange-correction functional, in which B3LYP functional was implemented (Becke f three-parameter hybrid HF/DFT exchange functional (B3)[40], and the Leeter hybrid HF/DFT exchange function (LYP)[41]). For the calculation, the 3-21G** basis set[42] with polarization functions was used giving 1449 basis functions per discussed molecule. The 3-21G** basis set was represented as a number of atomic orbitals composed of $M_{C,N,O}/M_H$ (3s2p/3s1p), consisting of 9 basis functions per C, N, O, P atoms and six basis functions per H atoms**.** All the calculations were performed with/according to convergence criteria of self-constructed fields equal to 10^{-6}. The calculations were performed in gaseous phase. For all performed calculations GAUSSIAN 03 Revision B.05 package was used[43]

Notes and references

[a]Food Science Department, Medical University of Lodz, Muszynskiego str. 1, 90-151 Lodz, Poland,

Tel: +48 42 677 91 41, e-mail: Bolek.Karwowski@wp.pl

[b]CEA, INAC, F-38000 Grenoble, France

[c]MRC/CRUK Oxford Institute of Radiation Oncology, University of Oxford, Old Road Campus Research Building, Roosevelt Drive, Oxford, OX3 7DQ, UK.

[d]Univ. Grenoble Alpes, INAC, F-38000 Grenoble, France.

† Electronic Supplementary Information (ESI) available: Figures of PAGE analysis, Tables with sequence of investigated oligonucleotides, Graphs of repair asay, selected bonds and dihedral angel flucuation. See DOI: 10.1039/b000000x/

Acknowledgements

We thank the EU for support through the Marie Curie Training and Mobility Project MRTN-CT2003 "CLUSTOXDNA".

Notes and references

1 A.G. Georgakilas, *Mol Biosyst,* 2008, **4**, 30-35

2 a) J. Cadet, J-L. Ravanat, M. Taverna-Porro, H. Menoni, D. Angelov, *Cancer Lett.,* 2012, 327, 5-15 ; b) L.J. Eccles, P. O'Neill, M.E. Lomax, *Mutation Res., 2011,* **711**, 134-141; c) A.G. Georgakilas, P. O'Neill, R.D. Stewart, *Radiat. Res*., 2013, **180**, 100-109 (2013)

3 J. Cadet, T. Douki, J-L. Ravanat, *Free Radic. Biol. Med.*, 2010, **49**, 9-21

4 J. Cadet, J.R. Wagner, Cold Spring Harb. *Perspect. Biol.*, 2013, 5, a012559

5 N. Belmadoui, F. Boussicault, M. Guerra, J-L. Ravanat, C. Chatgilialoglu, J. Cadet,*Org. Biomol. Chem.,* 2010, **8**, 3211-3219.

6 C. Chatgilialoglu, C. Ferreri, M.A. Terzidis,*Chem. Soc. Rev.*, 2011, **40**, 1368-1382

7 G.S. Madugundu, J.R. Wagner, J. Cadet, K. Kropachev, B.H. Yun, N.E. Geacintov, V. Shafirovich, *Chem. Res. Toxicol.*, 2013, **26**, 1031-1033

8 J. Cadet, J.R. Wagner, V. Shafirovich, N.E. Geacintov, *Int. J. Radiat. Biol.*, 2014, **90**, 423-436.

9 P. Regulus, B. Duroux, P.A. Bayle, A. Favier, J. Cadet, J-L. Ravanat, *Proc. Natl. Acad. Sci. USA.*, 2007, **104**, 14032-14037

10 A. Sancar, A.L. Lindsey-Boltz, K. Unsal-Kacmaz, S. Linn, *Ann. Rev. Biochem.*, 2004, **73**, 39-85

11 I. Kuraoka, C. Bender, A. Romieu, J. Cadet, R.D. Wood, T. Lindahl, *Proc. Natl. Acad. Sci. USA.*, 2000, **97**, 3832-3837

12 P.J. Brooks, D.S. Wise, D.A. Berry, J.V. Kosmoski, M.J. Smerdon, R.L. Somers, H. Mackie, A.Y. Spoonde, E.J. Ackerman, K. Coleman, R.E. Tarone, J.H. Robbins, *J. Biol. Chem.*, 2000,**275**, 22355-22362

13 K. Kropachev, S. Ding, M.A. Terzidis, A. Masi, Z. Liu, Y. Cai, M. Kolbanovskiy, C. Chatgilialoglu, S. Broyde, N.E. Geacintov, V. Shafirovich, *Nucleic Acids Res.*, 2014, **42**, 5020-5032.

14 J. Wang, H. Cao, C. You, B. Yuan, R. Bahde, S. Gupta, C. Nishigori , L.J. Niedernhofer, P.J. Brooks, Y. Wang, *Nucleic Acids Res.*, 2012, **40**, 7368-7374

15 A. Sancar, T.J.Reardon, *Adv.Protein Chem.*, 2004, **69**, 43-71

16 A.V. Semenko, D.R. Stevart, J.E. Ackerman, *Radiat. Res*. 2005, **164**, 180-193

17 D.T. Goodhead, *Int. J. Radiat. Biol.*, 1994, **65**, 7-17

18 Committee on Health Risks to Radon BEIR IV*, Effect of Exposure to* Radon, National Academy Press, Washington, DC, 1999

19 D.J. Brener, C.D. Eliston,*Radiology*, 2004, **232**, 735-738

20 a) M.H. David-Cordonnier, S.M. Cunniffe, I.D. Hickson, P. O'Neill, *Biochemistry*, 2002, **41**, 634-642; b)M.A. Chudhry, M. Weinfeld, *J. Biol. Chem.*, 1997, **272**, 15650-15655; c) M. Gulston, C. de Lara, T. Jenner, E. Davis, P. O'Neill, *Nucleic Acids Res.*, 2004, **32**, 1604-1609; d)J.O. Blaisdell, S.S. Wallace, *Proc. Natl. Acad. Sci.*, USA., 2001, **98**, 7426-7430

21 M.E. Lomax, S. Cunniffe, P. O'Neill, *Biochemistry*, 2004, **43**, 11017-11026

22 S.M. Cunniffe, M.E. Lomax, P. O'Neill, *DNA Repair* (*Amst*), 2007, **6**, 1839-1849.

23 S. Bellon, N. Shikazono, S. Cunniffe, M. Lomax, P. O'Neill, *Nucleic Acids Res.*, 2009, **37**, 4430-4440

24 T.E. Barrett, R. Savva, G. Panayotou, T. Barlow, J. Jiricny, L.H. Pearl, *Cell*, 1998, **92**, 117-129

25 E.H. Parikh, D.C. Mol, G. Slupphaug, S. Bharatii, E.H. Krokan, J.A. Tainer, *EMBO*, 1998, **17**, 5214-5226

26 a) M. Takeshita, C-N. Chang, F. Johson, S. Will, A.P. Grollman,*J. Biol. Chem.*, 1987, **262**, 10171-10179, J-B. Bertrand, J-J Vasseur, B. Rayner, J-L. Imbach, J. Paoletti, C. Paoletti, C. Malvy, *Nucleic Acids Res.*, 1989, **17**, 10308-10319; b) A.D. King, L. Zhang, R. Guarente, R. Marmorstein, *Nat. Struc. Biol.*, 1999, **6**, 22-27

27 W.K. Olson, M. Bansal, S.K. Burley, R.E. Dickerson, M. Gerstein, S.C. Harvey, U. Heinemann, X-J.Lu, S. Neidle, Z. Shakked, H. Sklenar, M. Suzuki, Ch-S.Tung, E. Westhof, C. Wolberger, H. M. Berman, *J. Mol. Biol.*, 2001, **313**, 229-237

28 H. Fujimoto, M. Pinak, T.Nemoto, P. O'Neill, E. Kume, K. Saito, H. Mekawa, *J. Comput. Chem.*, 2005, 12, 788-798

29 a) T. Zaliznyak, M. Lukin, C. de los Santos, *Chem. Res. Toxcol.*, *20*12, **25**, 2103–2111; B.T. Karwowski, *Comput. Theor.Chem.,*2013, **1010**, 38-44

30 A.Romieu, D. Gasparutto, D. Molko, J. Cadet, *J. Org. Chem.*, 1998, **63**, 5245-5249

31 M.H. David-Cordonnier, S. Boiteux, P. O'Neill.,*Biochemistry,* 2001, **40**, 11811-11818

32 A. Errami, V. Smider, W.K. Rathmell, D.M. He, E.A. Hendrickson, M.Z. Zdzienicka, G. Chu, *Mol. Cell.Biol.,* 1996, **16**, 1519-1536

33 P. Calsou, P. Frit, B. Salles, *J. Biol. Chem.* 1996, **271**, 27601-27607

34 M. Hashimoto, C.D. Donald, S.M. Yannone, D.J. Chen, R. Roy, Y.W. Kow, *J. Biol. Chem.,* 2001, **276**, 12827-12831.

35 HyperChemTMRelease 8.0.6 for Windows (temporary licence), Molecular Modeling System, Gainesville, FL 32601, USA.

36 W.D. Cornell, P. Cieplak, Ch.I. Bayly, I.R. Gould, K. M. Merz, D.M. Ferguson, D.C. Spellmeyer, T. Fox, J.W. Caldwell, P.A. Kollman, *J. Am. Chem. Soc.*, 1995, **117**, 5179–5197

37 a) E. Polak, Computatoinal methods in optimisation,auniified approach, Academy Press, 1971; b) G. Ribière, *Rev. Franç. Informat. Rech. Operationnelle*, 1969, **16**, 35-43

38 Accelrys DS Visualizer v2.0.1.7347, Accelrys Software Inc. Copyright ©2005-2007 (Freeware version).

39 a) G. Zheng, X-J. Lu, W.K. Olson, Web 3DNA - a web server for the analysis, reconstruction, and visualization of three-dimensional nucleic-acid structures, *Nucleic Acids Res.*, 2009, **37**(Web Server issue), W240-W246; b) X-J. Lu, W.K. Olson,*Nucleic Acids Res.*,2003, **31**, 5108-5121; c) X-J. Lu, W.K. Olson, *Nat Protoc.*, 2008., **3**, 1213-1227

40 A.D. Becke,*J. Chem. Phys.,*1993,**98**: 56481227t

41 C. Lee, W. Yang, R.G. Parr, *Phys. Rev. B, 1988,***37**, 7851988

42 J.S. Binkley, J.A. Pople, W.J. Hehre, *J. Am. Chem. Soc.*, 1980, **102**, 939–947

43 Gaussian 03 W, Revision D.01, M. J. Frisch, J. G. W. Trucks, H. B. Schlegel, G. E. Scuseria, M. A. Robb, J. R. Cheeseman, J. A. Montgomery, T. Vreven Jr., K. N. Kudin, J. C. Burant, J. M. Millam, S. S. Iyengar, J. Tomasi, V. Barone, B. Mennucci, M. Cossi, G. Scalmani, N. Rega, G. A. Petersson, H. Nakatsuji, M. Hada, M. Ehara, K. Toyota,R. Fukuda, J. Hasegawa,M. Ishida, T. Nakajima, Y. Honda, O. Kitao, H. Nakai, M. Klene, X. Li, J. E. Knox, H. P. Hratchian, J. B. Cross, V. Bakken, C. Adamo, J. Jaramillo, R. Gomperts, R. E. Stratmann, O. Yazyev, A. J. Austin, R. Cammi, C. Pomelli, J. W. Ochterski, P. Y. Ayala, K. Morokuma, G. A. Voth, P. Salvador, J. J. Dannenberg, V. G. Zakrzewski, S. Dapprich, A. D. Daniels, M. C. Strain, O. Farkas, D. K. Malick, A. D. Rabuck, K. Raghavachari, J. B. Foresman, J. V. Ortiz, Q. Cui, A. G. Baboul, S. Clifford, J. Cioslowski, B. B. Stefanov, G. Liu, A. Liashenko, P. Piskorz, I. Komaromi, R. L. Martin, D. J. Fox, T. Keith, M. A. Al-Laham, C. Y. Peng, A. Nanayakkara, M. Challacombe, P. M. W. Gill, B. Johnson, W. Chen, M. W. Wong, C. Gonzalez and J. A. Pople, Gaussian 03 Revision D.01, Gaussian, Inc., Wallingford CT, 2003.